

## Holographic and moiré aspherical compensators

J. García-Márquez, D. Malacara-Doblado, Z. Malacara-Hernández, and D. Malacara-Hernandez

*Centro de Investigaciones en Óptica, A.C.*

*Apartado postal 948, 37000 León, Guanajuato, Mexico*

*e-mail: jgarciam@foton.cio.mx*

Recibido el 3 de agosto de 1998; aceptado el 15 de febrero de 1999

Computer generated aspherical compensators are superimposed on an interferometer wavefront or fringe pattern to generate a null fringe pattern. This process has been understood and widely described in the literature. On the other hand, when we superimpose an ideal fringe pattern on top of the picture of an interferogram to be analyzed, we obtain a moiré pattern between the two images. These two apparently different procedures have much in common, but also some important differences to be described here.

*Keywords:* moiré; holography; interferometry

Un compensador esférico generado por computadora es superpuesto en el patrón de franjas de un interferómetro, a fin de generar un patrón de franjas nulo. Este proceso ya ha sido reportado ampliamente en la literatura. Por otro lado, cuando se superpone un patrón de franjas ideal sobre el negativo de un interferograma, se obtiene un patrón de franjas de moiré de estas dos imágenes. Aparentemente, estos dos métodos son muy similares, sin embargo, tienen diferencias que son importantes y que serán descritas en este artículo.

*Descriptores:* moiré; holografía; interferometría

PACS: 42.30.M; 42.40.J; 07.60.L

### 1. Introduction

Computer generated aspherical compensators can be superimposed on an aspheric wavefront or in the “live” fringe pattern in an interferometer to modify it and thus produce a null fringe pattern. This process has been widely described in the literature [1, 2]. On the other hand, when we superimpose an ideal fringe pattern on top of the picture of an interferogram to be analyzed, we obtain a moiré pattern between the two images. These two apparently different procedures have a lot in common, but also some important properties that we will describe.

An aspheric wavefront in a Mach-Zehnder, Fizeau or Twyman-Green interferometer produces non straight fringes with variable fringe spacings as shown in Fig. 1a. If the asphericity is strong, and the tilt is large enough to avoid closed fringes, the minimum fringe spacing may become of the order or smaller than the pixel period in the detector. Then, the sampling theorem limit is exceeded and, the need for an aspheric compensator arises. A computer generated holographic compensator may be used to eliminate the undesired spherical aberration of an aspheric wavefront to perform a null test of an aspherical surface, as proposed by several authors, like MacGovern and Wyant [3], Pastor [4], Wyant and Bennett [5] and described in detail by Creath and Wyant [1, 2].

The hologram is nothing else but an interferogram made with a large amount of tilt (a linear carrier), with a magnitude large enough to separate the diffracted compensated wavefront from the other orders of diffraction, as mentioned by

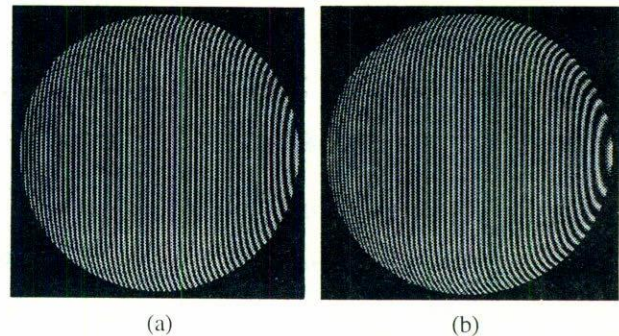


FIGURE 1. A Synthetic interferogram of an aspheric wavefront. a) With an aberrated aspherical wavefront and b) with an ideal aspherical wavefront.

Malacara and Malacara [6]. The wavefront compensation with a hologram can be made in a convergent or a collimated light beam. An example of a computer generated hologram used to eliminate the spherical aberration is shown in Fig. 1b. The tilt in this hologram is almost the same as that in the interferogram in Fig. 1a.

### 2. Theory

In the holographic compensator the ideal perfect wavefront under test is represented by

$$W(x, y) = A_W e^{i\phi(x, y)}, \quad (1)$$

where  $A_W$  can be considered a constant and  $\phi$  is the phase of the wavefront under test. This ideal wavefront under test

interferes with a flat reference wavefront  $R(x, y)$  given by

$$R(x, y) = A_R e^{i\alpha x}, \quad (2)$$

where again,  $A_R$  is a constant and  $\alpha = (2\pi/\lambda) \sin \theta$  and  $\theta$  is the wavefront inclination. Thus, the amplitude  $E(x, y)$  on the interference plane is

$$E(x, y) = W(x, y) + R(x, y), \quad (3)$$

and the irradiance on the hologram (interferogram) is

$$\begin{aligned} I(x, y) &= E(x, y)E^*(x, y) \\ &= A_W^2 + A_R^2 \\ &\quad + A_W A_R [e^{i(\phi(x, y) - \alpha x)} + e^{-i(\phi(x, y) - \alpha x)}], \quad (4) \end{aligned}$$

where the symbol \* stands for the complex conjugate. If the reconstructing wavefront is  $H(x, y)$  given by

$$H(x, y) = A_H e^{i\Phi(x, y)}. \quad (5)$$

Again  $A_H$  is a constant and  $\Phi$  is the phase of the reconstructing wavefront. Assuming a linear recording media, the transmission of the hologram may be considered to be directly proportional to the irradiance in Eq. (4). Thus, upon reconstruction we obtain

$$\begin{aligned} G(x, y) &= H(x, y)I(x, y) \\ &= (A_W^2 + A_R^2)A_H e^{i\Phi(x, y)} \\ &\quad + A_W A_R A_H [e^{i[\phi(x, y) + \Phi(x, y) - \alpha x]} \\ &\quad + A_W A_R A_H [e^{-i[(\phi(x, y) - \Phi(x, y) - \alpha x)]}]. \quad (6) \end{aligned}$$

It must be pointed out that these are the only terms present if we assume a linear recording of the hologram, thus producing sinusoidal fringes. However, a computer generated hologram produces higher order terms not considered here. This is the well known basic hologram theory. Let us now consider three different possible reconstructing schemes.

a) The first case of interest is when the illuminating (reconstructing) wavefront  $H(x, y)$  is identical to the flat reference wavefront, given by

$$H(x, y) = R(x, y), \quad (7)$$

thus obtaining

$$\begin{aligned} G(x, y) &= (A_W^2 + A_R^2)A_R e^{i\alpha x} + A_W A_R^2 e^{i\phi(x, y)} \\ &\quad + A_W A_R^2 e^{i[-\phi(x, y) + 2\alpha x]}. \quad (8) \end{aligned}$$

The first term represents the flat reference wavefront. The second term is the ideal reconstructed wavefront, which is to be compared with the wavefront under test. The third term is

a beam conjugate to the first order wavefront reproduced in the  $-1$  order of diffraction. This beam has opposite deformations to those of the first order. Since as pointed out before, the computer generated hologram is not formed by sinusoidal fringes, it has high order diffracted beams.

b) The second case to consider is when the illuminating (reconstructing) wavefront  $H(x, y)$  is close in shape to the perfect wavefront  $W(x, y)$ , but with a small difference in phase  $\Delta\phi(x, y)$  due to imperfections, as follows

$$\begin{aligned} H(x, y) &= W(x, y)e^{i\Delta\phi(x, y)} \\ &= A_W e^{i[\phi(x, y) + \Delta\phi(x, y)]}, \quad (9) \end{aligned}$$

then, the wavefronts generated by the interferogram are

$$\begin{aligned} G(x, y) &= (A_W^2 + A_R^2)A_W e^{i[\phi(x, y) + \Delta\phi(x, y)]} \\ &\quad + A_W^2 A_R e^{i[2\phi(x, y) + \Delta\phi(x, y) - \alpha x]} \\ &\quad + A_W^2 A_R e^{i[\Delta\phi(x, y) + \alpha x]}. \quad (10) \end{aligned}$$

The first term is the illuminating wavefront. The second term has an asphericity with twice the original magnitude, but with the small deformation of the reconstructing wavefront superimposed. The flat reference wavefront is reproduced only if this wavefront under test is perfect. Otherwise, any deviation from the ideal shape appears on the almost flat wavefront.

c) A third case to consider is when the hologram is illuminated with a wavefront  $H(x, y)$  with an asphericity with the opposite sign to the wavefront under test and the small deformation superimposed on it. Thus

$$\begin{aligned} H(x, y) &= W^*(x, y)e^{i[\Delta\phi(x, y) + 2\alpha x]} \\ &= A_W e^{i[-\phi(x, y) + \Delta\phi(x, y) + 2\alpha x]}. \quad (11) \end{aligned}$$

where \* denotes the complex conjugate, obtaining the following diffracted beams

$$\begin{aligned} G(x, y) &= (A_W^2 + A_R^2)A_W e^{i[-\phi(x, y) + \Delta\phi(x, y) + 2\alpha x]} \\ &\quad + A_W^2 A_R e^{i[\Delta\phi(x, y) + \alpha x]} \\ &\quad + A_W^2 A_R e^{i[-2\phi(x, y) + \Delta\phi(x, y) + 3\alpha x]}. \quad (12) \end{aligned}$$

where the first beam is the illuminating zero order. The second term is an almost flat wavefront. The third term is a wavefront not shown in Fig. 4a.

The spectral bandwidths of these beams are directly proportional to the maximum wavefront slope on these wavefronts that, is directly proportional to the maximum interferogram spatial frequency when the tilt is removed. Thus, the bandwidths would increase with their asphericities. Of course, these relative irradiances depend on the fringe profiles.

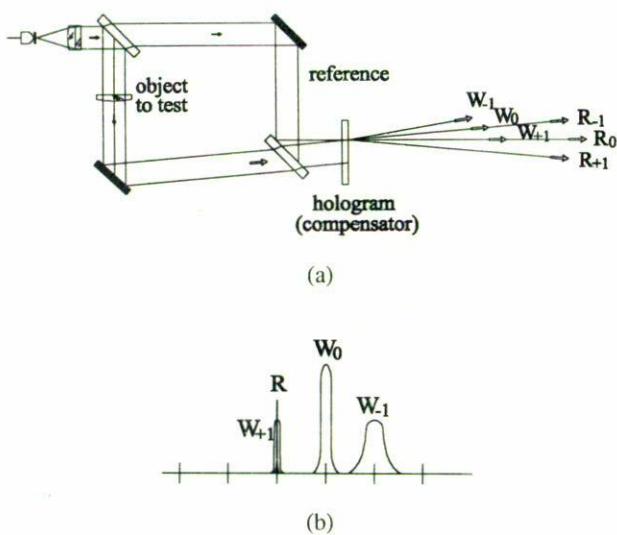


FIGURE 2. (a) Optical configuration with the hologram inside the interferometer cavity, and (b) spectra of wavefronts.

### 3. Holographic and Moiré compensators

The relation between holographic and Moiré compensators has been described before [6]. The compensating hologram can be used in three different manners, according to its location in the interferometer. These three manners, which are not the three configurations described in the preceding section, will be described using a Mach-Zehnder interferometer as an example. However, the same principles apply for Fizeau and Twyman-Green interferometers.

#### 3.1. Hologram inside the interferometer cavity

The compensating hologram may be placed in the path of the aberrated wavefront, inside the interferometer cavity, without disturbing the reference wavefront  $R$ , as in Fig. 2a. Then, the interferogram to be analyzed is formed by the interference between the wavefront under test, after being compensated by the hologram  $W_{+1}$  and the reference wavefront  $R$ . A total of four wavefronts are produced, the two interfering wavefronts and two extra ones that can be easily low pass filtered, since they travel in different directions and hence different spatial frequencies. This filtering can be performed in the image space by means of common convolution filters using masks or in the Fourier space by means of properly located pinholes.

The spectra of these wavefronts with their relative frequency separations are illustrated in Fig. 2b. The lobe of  $W_0$  should not overlap those of  $W_{+1}$  and  $R$ . Thus, the minimum linear carrier should be such that the lobes separation is larger than half the width of  $W_0$ .

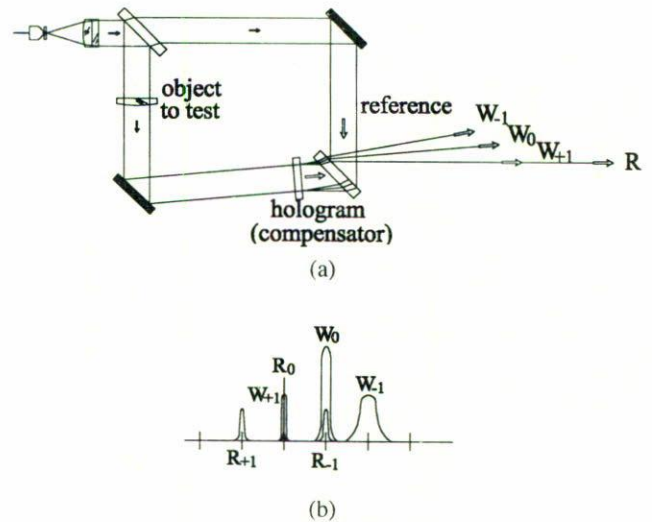


FIGURE 3. (a) Optical configuration with hologram outside the interferometer cavity and (b) spectra of wavefronts.

#### 3.2. Hologram outside the interferometer cavity

Another possibility is to place the hologram outside the interferometer cavity, in the path of both the wavefront under test and the reference beam, as illustrated in Fig. 3a. Then, both beams will pass through the hologram and reconstruct their own set of wavefronts. The interference now takes place between the zero order (undiffracted) of the reference beam  $R_0$  and the wavefront under test, after being compensated by the hologram  $W_{+1}$ . There are six wavefronts, the two interfering wavefronts and four more that should be filtered out. As in the preceding case, the low pass filtering can be performed in the image space as well as in the Fourier space.

The spectra of these wavefronts with their relative frequency separations are illustrated in Fig. 3b. The minimum linear carrier is the same as in the preceding case.

#### 3.3. Hologram in front of the interferogram picture

Still another possibility is to take a picture of the interferogram with any two wave interferometer, introducing a linear carrier by tilting one of the two wavefronts, and then illuminating it with a collimated beam of light as shown in Fig. 4a. Then, the transparency of the interferogram acts as a diffracting hologram, generating three wavefronts. One of the interfering wavefronts is the ideal aspheric wavefront produced by the non diffracted beam (zero order) in the interferogram, but diffracted by the compensating hologram. The other interfering wavefront is the wavefront to be measured, produced by diffraction on the interferogram (+1 order) but undiffracted by the compensating hologram (zero order). Besides these two interfering wavefronts, there are seven more, making a total of nine wavefronts. As before, the seven extra undesired wavefronts travel in different directions, thus, with different spatial frequencies. Therefore these wavefronts can also be eliminated by low pass filtering in the image space or in the

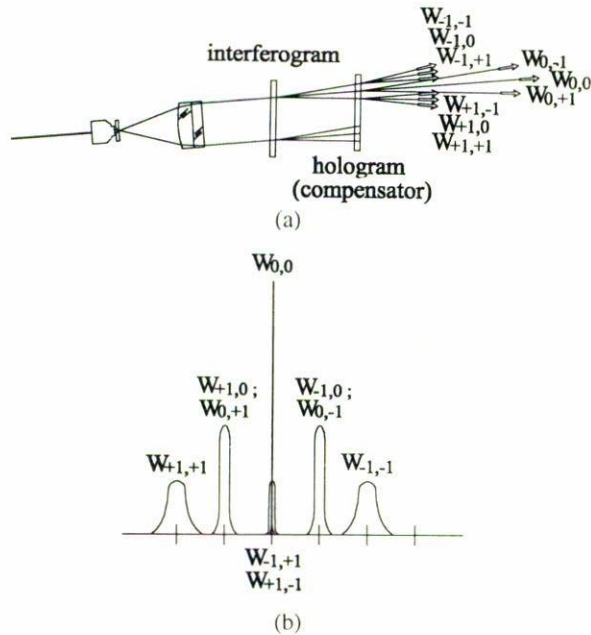


FIGURE 4. (a) Optical configuration with the hologram in front of the interferogram picture and (b) spectra of wavefronts.

Fourier space. The Fourier spectrum for this case is in Fig. 4b. The minimum linear carrier is the same as in the other two cases.

These method to compensate with a hologram has traditionally been considered a moiré process between the actual interferogram and the ideal interferogram. It is however quite interesting to see that it is really a compensating process with a hologram.

#### 4. Demodulating an interferogram with a linear carrier

When analyzing an interferogram to extract the wavefront shape, a phase shifting method is the ideal if an interpolation procedure is to be avoided. Otherwise, if the fringe positions are sampled, the relatively large spacing between the fringes make absolutely necessary a polynomial interpolation, with the well known limitations.

Alternatively, a solution proposed by several researchers to avoid phase shifting, is the introduction of a large linear carrier (a large tilt). Womack [7] proposed a method to demodulate the interferogram in the image space using a method similar to the demodulation procedures used in electronic communications, in order to obtain the phase information (wavefront deformations). On the other hand, Takeda *et al.* [8] proposed a method of demodulation in the Fourier space.

Both demodulations schemes are very powerful, with different advantages and disadvantages. A basic requirement is that the linear carrier should be of a magnitude large enough to avoid closed fringes. This condition can be expressed by saying that the minimum linear carrier should be such that

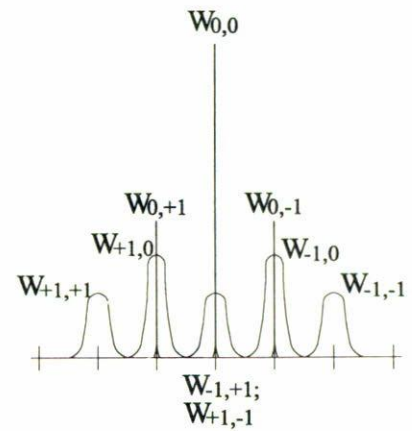


FIGURE 5. Spectrum when demodulating an interferogram with a linear spatial carrier using moiré with a linear ruling.

the separation between lobes in the Fourier space is larger than half the width of the wide lobe.

The main disadvantage of these methods is the large amount of mathematics and image digitization methods involved. Let us assume that the interferogram linear carrier has to be removed in order to obtain a qualitative assessment of the wavefront. If the wavefront has not been frozen, that is the picture has not been taken, the tilt can very easily be removed in the interferometer by tilting one of the mirrors. However, if the picture is already taken, the only alternative to remove the linear carrier is by moiré with a linear ruling with the same frequency as the linear carrier. This last procedure is basically the same already described here. The only difference is that the compensating hologram is now a linear ruling. Thus, we have nine diffracted wavefronts as in Fig. 4a with a spectrum for these wavefronts as in Fig. 5.

It is interesting to see that the minimum linear carrier to be able to filter the desired wavefronts is when the side lobes just touch the central lobes. It is easy to see now that the minimum linear carrier is that which gives a separation between the lobes equal to the width of the lobes. Thus, the minimum linear carrier in order to use moiré visual demodulation is twice the minimum linear carrier using Womack's or Takeda's demodulation methods. This is an unexpected result.

#### 5. Conclusion

Interferogram analysis with holographic compensators and with the moiré fringe patterns produced by comparison with a reference grating are essentially the same methods, with small but interesting differences as described before.

It has been shown that, there are three possible ways of measuring an aspheric wavefront using hologram compensators, depending on the position of holographic compensator. These methods are basically the same method, but have some important practical differences that can decide which method is best in a given case.

The theoretical and conceptual differences between demodulating an interferogram with a linear carrier using digitalization and mathematical procedures and the analog moiré demodulation method had been pointed out.

## Acknowledgments

The research grant from CONACyT to carry on this project is gratefully acknowledged.

- 
1. K. Creath and J.C. Wyant, "Holographic and Speckle Tests", in *Optical Shop Testing*, Second edition, edited by D. Malacara, (John Wiley & Sons, Inc., New York, 1992) Chapt. 15.
  2. K. Creath and J.C. Wyant, "Moiré and Fringe Projection Techniques", in *Optical Shop Testing*, Second edition, edited by D. Malacara, (John Wiley & Sons, Inc., New York, 1992b) Chapt. 16.
  3. A.J. MacGovern and J.C. Wyant, *Appl. Opt.* **10** (1971) 619.
  4. J. Pastor, *Appl. Opt.* **8** (1969) 525.
  5. J.C. Wyant and V.P. Bennett, *Appl. Opt.* **11** (1972) 2833.
  6. D. Malacara and Z. Malacara, *Proc. SPIE.* **2553** (1995) 382.
  7. K.H. Womack, *Opt. Eng.* **23** (1984) 391.
  8. M. Takeda, I. Hideki, and S. Kobayashi, *J. Opt. Soc. Am.* **72** (1982) 156.